Identification of novel antioxidant peptides from snakehead (*Channa argus*) soup generated during gastrointestinal digestion and insights into the anti-oxidation mechanisms

Jin Zhang [a, b]; Mei Li [d, e]; Gaonan Zhang [a]; Yu Tian [e]; Fanbin Kong [c]; Shanbai Xiong [a, f]; Siming Zhao [a, f]; Dan Jia [g]; Anne Manyande [h]; Hongying Du [a, f*]

[a] College of Food Science and Technology, Huazhong Agricultural University, Wuhan, Hubei 430070, P. R. China;

[b] Institute of Food Science, Zhejiang Academy of Agricultural Sciences, Hangzhou, Zhejiang 310021, P. R. China;

[c] Department of Food Science and Technology, The University of Georgia, Athens, GA 30602, USA;

[d] CAS Key Laboratory of Brain Connectome and Manipulation, the Brain Cognition and Brain Disease Institute (BCBDI), Shenzhen Institutes of Advanced Technology; Chinese Academy of Sciences, 518055, P. R. China

[e] State Key Laboratory of Magnetic Resonance and Atomic and Molecular Physics, Key Laboratory of Magnetic Resonance in Biological Systems, Wuhan Institute of Physics and Mathematics, Innovation Academy for Precision Measurement Science and Technology, Chinese Academy of Sciences, Wuhan, Hubei 430071, P. R. China

[f] National R & D Branch Center for Conventional Freshwater Fish Processing, Wuhan, Hubei 430070, P. R. China

[g] College of Animal Science and Technology, Yunnan Agricultural University, Kunming, Yunnan 650201, P. R. China

[h] School of Human and Social Sciences, University of West London, Middlesex, TW89GA, UK

Running title: Antioxidant peptides from freshwater fish

[*] Corresponding author: Hongying Du, Associate Professor.

College of Food Science and Technology, Huazhong Agricultural University, No.1 Shizishan Street, Wuhan, Hubei 430070, P. R. China. Tel & Fax: +86-27-87288375; E-mail: hydu@mail.hzau.edu.cn

Abstract: Antioxidant peptides obtained from snakehead (*Channa argus*) soup (SHS) after simulated gastrointestinal (GI) digestion were separated, identified and characterized. Results showed that the fraction with MW < 3 kDa had the highest antioxidant capacity. Four novel antioxidant peptides were identified after RP-HPLC and UPLC-MS/MS. PGMLGGSPPGLLGGSPP and SDGSNIHFPN had the highest DPPH radical scavenging activity (IC_{50} = 1.39 mM) and Fe^{2+} chelating ability (IC_{50} = 4.60 mM), respectively. Structures *in silico* for IVLPDEGK, PGMLGGSPPGLLGGSPP and SDGSNIHFPN suggest that at least one β-turn and/or α-helix, are associated with antioxidant activity. Moreover, our results showed that these three peptides docked with a recombinant Kelch-like ECH-associated protein 1 (Keap1) with a binding score greater than TX6, a good ligand of Keap1. The cell viability assay also showed significant cytoprotective effects against H_2O_2-induced cellular oxidative damage. This information implies that antioxidant mechanisms of novel peptides occurred via activation of cellular anti-oxidation Keap1-Nrf2 signaling pathway.

Keywords: antioxidant peptides; snakehead soup; gastrointestinal digestion; molecular docking; UPLC-MS/MS; RP-HPLC; Kelch-like ECH-associated protein 1; cytoprotective effect

1. Introduction

Snakehead (*Channa argus*) is a traditional, high-value, freshwater fish species indigenous to Asia-Pacific countries such as China and Malaysia (Wahab et al., 2015; Wu, Zhang, Huo, Xiong, & Du, 2018), and its annual aquaculture production exceeded 0.48 million tons in 2018 in China (China Fishery Statistical Yearbook, 2019). Snakeheads contain few bones, which means the edible portion makes up 63%, and like many fish, is rich in high-quality protein and micronutrients (Wu et al., 2018). Due to its high levels of essential amino acids and fatty acids, snakeheads are usually used as ingredients in soup, a popular side dish in Asia-Pacific countries (Sahid et al., 2018; Zhang, Zheng, Feng, Shen, Xiong, & Du, 2018). Moreover, snakehead fish has been reported to significantly promote the healing of wounds and burns (Sahid et al., 2018).

The wound repair process could induce cellular oxidative stress, producing various types of free radicals, which severely interfere with wound healing (Schäfer & Werner, 2008). Many previous studies have reported that the wound healing promotion potency of fish and fish products may mainly be derived from their released antioxidant peptides (Wang, Doan, Nguyen, Nguyen, & Wang, 2019; Venkatesan, Anil, Kim, & Shim, 2017). Antioxidant peptides can protect the human body against cellular oxidative stress by scavenging reactive oxygen species, chelating transition metal and inhibiting lipid peroxidation (Delgado, Nardo, Pavlovic, Rogniaux, Añón, & Tironi, 2016; Sila & Bougatef, 2016). Their antioxidant activity is closely related to the molecular weight (MW), hydrophobicity, amino acid residue composition and folding pattern (Delgado et al., 2016). Our previous study found an increase in antioxidant activity of SHS during gastrointestinal (GI) digestion (Zhang et al., 2018). However, the antioxidant peptides from snakehead fish have rarely been studied, and the antioxidant peptides generated and released from SHS during digestion have not been reported

yet.

Although the *in vivo* antioxidant mechanism of peptides is still not fully understood, various reports have indicated that the Keap1-Nrf2 anti-oxidation signaling pathway is one of the most probable approaches (Han et al., 2018; Huerta et al., 2016; Li et al., 2017). This pathway is an important regulator of cytoprotective responses to oxidative stress (Magesh, Chen, & Hu, 2012). In this pathway, the transcription factor Nrf2 (nuclear factor erythroid 2-related factor 2) is a key factor involved in the cellular anti-oxidation process, while the repressor protein Keap1 (Kelch-like ECH-associated protein 1) promotes the degradation of Nrf2 (Zhang, Lo, Sun, Habib, Lieberman, & Hannink, 2005). Therefore, external molecules that can bind to Keap1 and inhibit the Keap1-Nrf2 complex formation would enhance the *in vivo* antioxidant activity (Li et al., 2017). However, it is still not clear whether the antioxidant activity of peptides from SHS is associated with the Keap1-Nrf2 signaling pathway. Such potential interactions between peptides and Keap1 can be evaluated through the use of *in silico* molecular docking and cell model.

Therefore, the objective of this study was to separate, identify and characterize antioxidant peptides from SHS generated by GI digestion. Ultrafiltration and reversed-phase high-performance liquid chromatography (RP-HPLC) were used to separate antioxidant peptides. Ultra-high pressure liquid chromatography coupled with mass spectrometry (UPLC-MS/MS) and 3D structure *in silico* prediction were utilized to identify the sequences and characterize the structures of these novel antioxidant peptides. The molecular docking technology and HepG2 cell model were also adopted for understanding their *in vivo* antioxidant mechanism. The information obtained from the present study could help our understanding of the antioxidant mechanism of SHS and provide theoretical support for the high-value utilization of freshwater fish products.

2. Materials and methods

2.1. Materials

Fresh snakeheads (*C. argus*, approximately ~750 g per fish, n = 20) were purchased from a local market in Wuhan, China and taken to the laboratory in a plastic bag within 20 min. 1,1-diphenyl-2-picrylhydrazyl (DPPH), 1,10-phenanthroline monohydrate, ferrozine, trichloroacetic acid (TCA), glutathione (GSH), lysozyme, L-tyrosine (L-Tyr), bovine serum albumin (BSA), vitamin B12 (VB12), vitamin C (VC) and ethylenediaminetetraacetic acid (EDTA) were bought from China National Medicines Co., Ltd. (Beijing, China). Sephadex G-25 was obtained from Sigma-Aldrich Co., Ltd. (St. Louis, MO, USA). HepG2 cells were acquired from the Beijing Institute of Biochemistry and Cell Biology (Beijing, China). All other reagents used were analytical grade, including pepsin (3000-3500 National Formulary Unit/mg, BIOSHARP, St Louis, MO, USA) and pancreatin (4000 U/g, Yuanye Biotechnology Co., Ltd., Shanghai, China).

2.2. Preparation and simulated gastrointestinal (GI) digestion of snakehead soup (SHS)

The fresh snakehead, with scales, branchia, and offal removed, was rinsed several times before use. The fish was immersed in water at a ratio of 1:4 (w/v) and then cooked using an induction cooker (RT2134, Midea group, Foshan, China). The cooking power was 500 W for the first 20 min until the sample soup started to boil, and then reduced to 300 W and kept boiling for 70 min. The soup was then filtered through six layers of gauze to remove solids.

Subsequently, the simulated GI digestion of SHS was performed using a two-step enzymatic process according to the method of Zheng, Ren, Su, Yang, & Zhao. (2013) and Zhu, Zhang, Zhou, &

111 Xu. (2016) with minor modifications. The soup sample was adjusted to pH 2.0 with 1 M HCl, and
112 pepsin was then added to a level of 40 g/kg of the protein content, which was determined by the
113 method of Lowry, Rosebrough, Farr, & Randall. (1951). The mixture was blended and incubated at
114 37 °C for 2 h with shaking at a speed of 100 rpm (COS-100B, Bilon Instruments Co., Ltd., China) to
115 simulate gastric digestion. Subsequently, the mixture was adjusted to pH 5.3 using 0.9 M $NaHCO_3$ and
116 then to pH 7.5 with 1 M NaOH. Pancreatin was then added at 40 g/kg of the protein content and the
117 reaction mixture was further incubated at 37 °C for 2.5 h to simulate intestinal digestion. Then test
118 tubes were placed in boiling water for 10 min to terminate the digestion. Samples were then cooled to
119 room temperature and centrifuged at 16,000 × *g* for 20 min (TGL-16GA, Xingkekeji, Instruments Co.,
120 Ltd., Changsha, China). The supernatant was filtrated and then freeze-dried (ALPHA 1-4 LD, Martin
121 Christ, Osterode, Germany) for the separation of antioxidant peptides.
122
123 *2.3. Measurement of peptide molecular weight (MW) distribution*
124 The peptide MW distribution of SHS after simulated GI digestion was purified by gel filtration
125 chromatography. The Sephadex G-25 column (1.6 cm × 70 cm) was loaded and eluted with 0.02%
126 NaN_3 for 12 h until reaching equilibration. 1 mL 10 mg/mL GI digested sample solution was then
127 added into the pre-equilibrated column and eluted at a flow rate of 16 mL/h with 0.02% NaN_3 at room
128 temperature. The elution was collected at 15 min intervals and assayed at 280 nm with a UV-1750
129 spectrophotometer (Shimadzu, Kyoto, Japan). GSH, lysozyme, L-Tyr, BSA and VB_{12} were used as the
130 standard substances of this measurement. The relationship between lg (MW) of each substance and the
131 occurrence time of the corresponding maximum absorption peak was drawn as the standard curve.
132

2.4. Separation of antioxidant peptides

2.4.1. Ultrafiltration

SHS samples collected from simulated GI digestion were ultrafiltered sequentially using Amicon Ultra-15 centrifugal filters with 10 kDa and 3 kDa MWCO (Millipore, Bedford, MA, USA). All recovered fractions (SHS-I, MW > 10 kDa; SHS-II, 3-10 kDa; SHS-III, MW < 3 kDa) were freeze-dried and stored at -80 °C for use. Their antioxidant activities were determined as described in Section *2.5* and compared with the original simulated GI digested SHS sample and its different fractions.

2.4.2. Reversed-phase high performance liquid chromatography (RP-HPLC)

According to the method of Shen, Chahal, Majumder, You, & Wu. (2010) with some modifications, the fractions with the highest antioxidant activity were investigated using an Agilent 1260 semi-preparative HPLC instrument (Agilent Technologies Inc., Santa Clara, CA, USA) equipped with a reversed-phase Techmate ST C18 analytical column (5 μm, 150 mm × 4.6 mm) (Techmate Technology Co. Ltd., Beijing, China). The gradient elution was conducted at a flow rate of 0.2 mL/min with 20 mM ammonium formate in deionized water (pH = 10, adjusted with ammonium hydroxide) as elution A and 20 mM ammonium formate in 80% acetonitrile solution added with equivalent 25% ammonium hydroxide as elution B. The column was maintained at room temperature. The elution was collected at 3 min intervals and assayed at 216 nm. Ultimately, 10 fractions (F1-F10) were collected and their DPPH radical scavenging activities were detected as described later. Then fractions were freeze-dried for further studies.

155 *2.5. Evaluation of antioxidant activity of peptides*

156 *2.5.1. DPPH radical scavenging activity*

157 The DPPH radical scavenging activity was determined according to the method of Zhang, Li,
158 Miao, & Jiang. (2011) with minor modifications. Specifically, a 4 mL sample was mixed with 1 mL
159 0.1 mM DPPH solution (in 99.7% ethanol); the control group comprised of 4 mL sample solution
160 mixed with 1 mL 99.7% ethanol; and the blank group contained 4 mL deionized water mixed with 1
161 mL 0.1 mM DPPH (in 99.7% ethanol). The mixture was blended and kept in the dark for 30 min at
162 room temperature. Subsequently, the absorbance of the reaction mixture was detected at 517 nm. The
163 DPPH radical scavenging activity was calculated according to the following equation:

164 $$\text{DPPH radical scavening activity (\%)} = [1 - (A_s - A_b) / A_c] \times 100\% \quad \text{(Eq. 1)}$$

165 where *As*, *Ab* and *Ac* represent the absorbance of the sample group, blank group and control group,
166 respectively.

167

168 *2.5.2. Hydroxyl radical scavenging activity*

169 The hydroxyl radical scavenging activity was measured using the method of Li, Jiang, Zhang, Mu,
170 & Liu. (2008) with some modifications. Briefly, a reaction mixture solution was composed of 2 mL
171 sample mixed with 1 mL 0.75 mM 1,10-phenanthroline, 1 mL 0.75 mM $FeSO_4$ and 2 mL 0.2 M
172 phosphate buffer (pH = 7.4). Then 1 mL 0.12% H_2O_2 solution was added to the mixture and incubated
173 at 37 °C for 1 h, and the absorbance was detected at 536 nm. The control group comprised of the same
174 solutions as the sample group, except that equivalent deionized water was used instead of the sample
175 solution. The composition of the blank group was the same as that of the sample group, except that
176 equivalent deionized water was used instead of the 1,10-phenanthroline monohydrate and $FeSO_4$

177 solutions. The hydroxyl radical scavenging activity was determined using the equation shown as
178 follows:

179 $$\text{OH radical scavening activity (\%)} = (A_s - A_c) / (A_b - A_c) \times 100\% \quad \text{(Eq. 2)}$$

180 where *As*, *Ab* and *Ac* represent the absorbance of the sample group, blank group and control group,
181 respectively.

182

183 *2.5.3. Fe^{2+} chelating ability*

184 The Fe^{2+} chelating ability was measured as described by Decker & Welch (1990) with slight
185 modifications. Specifically, the sample group comprised of 1 mL sample solution mixed with 3.7 mL
186 deionized water, 0.1 mL 2 mM $FeCl_2$ and 0.2 mL 5 mM ferrozine. The mixture was blended and kept
187 at room temperature for 20 min, and then the absorbance was detected at 562 nm. The deionized water
188 was used as the control, while the deionized water instead of $FeCl_2$ and ferrozine was used for the
189 blank. The chelating ability of Fe^{2+} was determined by the following equation:

190 $$Fe^{2+} \text{ chelating ability (\%)} = [1 - (A_s - A_b) / A_c] \times 100\% \quad \text{(Eq. 3)}$$

191 where A_s, A_b and A_c represent the absorbance of the sample group, blank group and control group,
192 respectively.

193

194 *2.5.4. Reducing power*

195 The reducing power was determined by the method of Oyaizu (1986) with some modifications. 2
196 mL sample solution and 2 mL 0.2 M phosphate buffer (pH = 6.6) were mixed with 2 mL 1% K_3Fe
197 $(CN)_6$. The mixture was blended and incubated at 50 °C for 20 min and then mixed with 2 mL 10%
198 TCA, followed by centrifugation at 1750 × *g* for 10 min. Then 2 mL supernatant was added with 2 mL

deionized water and 0.4 mL 0.1% $FeCl_3$. Subsequently, the reaction mixture was blended thoroughly and kept at room temperature for 10 min before the absorbance detection of the resulting Prussian blue at 700 nm.

2.6. UPLC-MS/MS-based peptide identification

The collected fractions with the highest DPPH radical scavenging activity were then sequenced using a UPLC-MS/MS system. All experiments were performed on a triple time-of-flight (Triple TOF) System (5600 plus, AB SCIEX, Foster City, CA, USA) coupled with a splitless ultra-high pressure liquid chromatography (UPLC) system (Ultra 1D Plus, Eksigent, Dublin, CA, USA). After desalting with Sephadex G-25, the peptides were dissolved in 0.1% formic acid mixed with 2% acetonitrile and 98% deionized water, and then loaded into a C18 trap column (5 μm, 5 × 0.3 mm, Agilent Technologies, Inc., Santa Clara, CA, USA) at a flow rate of 5 μL/min. Subsequently, it was eluted from the trap column over the C18 analytic column (75 μm × 150 mm, 3 μm particle size, 100-Å pore size, Eksigent, Dublin, CA, USA) at a flow rate of 300 nL/min in a 100 min gradient. The information-dependent acquisition mode was used to acquire MS/MS spectra. Survey scans were acquired in 250 ms and 40 product ion scans were collected in 50 ms/scan. The precursor ion range was set from m/z 350 to m/z 1500, and the product ion range was set from m/z 100 to m/z 1500.

Raw data from the MS/MS system were analyzed using the ProteinPilot 4.5 software. The protein accession and sequence location were achieved by comparing mass data against the UniProt database (http://www.uniprot.org/) at the conditions of "identified sample type, no cysteine alkylation, and thorough search effort". Meanwhile, according to the method outlined by Sheng et al. (2019) and Zhang et al. (2020), sequences with abundance in the MS/MS spectra above 1.00×10^7 were selected

for further analysis because they were easy to detect. Moreover, the peptides with sequencing confidence ≥ 85% were further selected and considered as the finally identified antioxidant peptides.

2.7. Synthesis and antioxidant activity of identified peptides

Identified antioxidant peptides were synthesized by the solid-phase procedure using the Fmoc-protected amino acid synthesis method. The peptide synthesis was conducted by Dechi Biosciences Co., Ltd. (Shanghai, China). The obtained peptides showed a purity higher than 95% (w/w) detected by RP-HPLC on conditions of mobile phase A, 0.1% TFA in water; mobile phase B, 0.1% TFA in acetonitrile; flow rate, 1 mL/min; column, Kromasil-C18, 5 μm particle size, 250 mm × 4.6 mm (Eka Nobel, Bohus, Sweden). The molecular masses of synthesized peptides were determined with the MS system. The DPPH radical scavenging activity and Fe^{2+} chelating ability of synthesized peptides at different concentrations (0-2 mg/mL) were assayed as described above. The half-maximal inhibitory concentration (IC_{50}) of the peptide was obtained by non-linear regression analysis fitted to a sigmoidal dose-response equation.

2.8. Three-dimensional (3D) structure in silico prediction of identified peptides

The 3D structure models of identified peptides were predicted using the PEP-FOLD tool V3.5 (http://bioserv.rpbs.univ-paris-diderot.fr/services/PEP-FOLD3/), a *de novo* resource aimed at predicting peptide structures from amino acid sequences (Lamiable, Thévenet, Rey, Vavrusa, Derreumaux, & Tufféry, 2016). The folding pattern calculated with the lowest energy was selected as the conformation of peptides generated by the PEP-FOLD tool V3.5. Images and analysis of the 3D structures were generated using the Discovery Studio software 2016 (Accelrys Software Inc., San

Diego, CA, USA).

2.9. Molecular docking analysis

The molecular docking of identified peptides with Keap1 was conducted following the methods provided in Han et al. (2018) and Li et al. (2017) with minor modifications. The semi-flexible program CDOCKER in the Discovery Studio software 2016 was used for this procedure. Before the docking, the crystal structure of human Keap1 (PDB ID: 2FUL) was downloaded from the PDB database and pretreated with the Prepare Program in Discovery Studio to build loops, minimize the energy, remove water molecules, remove Nrf2 16-mer peptide and protonize. The docking pocket was defined based on the active sites of Keap1 as x: 5, y: 9, z: 1 and radius: 15 Å (Li et al., 2017). Furthermore, the TX6 (PubChem Compound ID: 121488089) was used as the reference ligand since it showed strong binding capacity with Keap1 and activated the Nrf2 pathway (Huerta et al., 2016). Meanwhile, the identified antioxidant peptides were also minimized in energy. The docking program was performed with the partial flexibility CDOCKER protocol, specifically, the receptor (Keap1) was set as rigid and the ligands (the identified peptides or TX6) were set as flexible. The molecular docking results were evaluated based on the –CDOCKER interaction energy (–CIE) score, interaction site, and interaction fore types with Keap1.

2.10. Cytoprotective effects against cell damage induced by H_2O_2

The identified antioxidant peptides with successful molecular docking performance were selected and their cytoprotective effects were evaluated using cell viability assay. Briefly, HepG2 cells were cultivated in a humidified atmosphere (37 °C, 5% CO_2) with DEME medium (containing 10% fetal bovine serum and 1% penicillin-streptomycin). To determine the cytotoxicity of the synthetic peptides

(125-1000 μM) on HepG2 cells, the cells were seeded in a 96-well plate at a concentration of 1.0×10^4 cells/well. After 24 hours, cells were incubated with different concentrations of the synthetic peptides for another 24 hours. Then, cell survival was determined by the MTT (3-(4,5-dimethyl-2thiazolyl)-2,5-diphenyl-2-H-tetrazolium bromide) assay. The protective effects of the synthetic peptides (125-1000 μM) on HepG2 cells were appraised by establishing a H_2O_2-induced (350 μg/mL) oxidative stress model. Briefly, HepG2 cells (1.0×10^4 cells/mL) were seeded in culture plates at 37 °C for 24 h. The experiment was divided into five different groups, including the blank group (100 μL cell suspension), oxidative damage group (100 μL H_2O_2 solution), low-concentration peptide-protected group (50 μL H_2O_2 and 50 μL peptide solution), medium-concentration peptide-protected group (50 μL H_2O_2 and 50 μL peptide solution) and high-concentration peptide-protected group (50 μL H_2O_2 and 50 μL peptide solution). The cell viability was determined by absorbance at 570 nm using a microplate reader.

2.11. Statistical analysis

All experiments were performed in triplicate. Tables were made by Microsoft Excel 2016 while figures were drawn using Origin V8.0 and Microsoft PowerPoint 2016. Analysis of variance and regression were conducted using the SAS program V8 (SAS Institute Inc., Carry, NC, USA). Differences among mean values were established using the Duncan multiple range test. The significant difference was confirmed when $P < 0.05$.

3. Results and Discussion

3.1. MW distribution of peptides from simulated GI digested SHS

The peptide MW distribution of simulated GI digested SHS is shown in Fig. 1a and the fitted linear equation between lg (MW) (y) and elution time (x) were calculated by the method of least square as y = -0.0106 x+ 6.2445 (R^2=0.9733) (Fig. 1b). It can be seen from Fig. 1a that four main fractions (F-I to F-IV) differed in MW range derived from simulated GI digested SHS. F-I was approximately 20-kDa or larger and accounted for about 7.36% of the whole GI digesta. It was considered as less completely digested if macromolecular proteins consisted of several hundreds of amino acid residues. F-II contained the least component (14.68% of the whole digesta) with MW of 3.5-21.7 kDa, indicating that it had mainly peptides containing several tens of amino acid residues. At last, the rest (about 77.96%) of the whole digesta was distributed in two fractions with MW < 3 kDa. F-III had MW of 400-2,400 Da, demonstrating that this fraction was mainly short-chain peptides with 3-20 amino acid residues. F-IV accounted for the maximal proportion and possessed MW < 400 Da with a sharp peak. This fraction is probably comprised of dipeptides and free amino acids. Tyrosine (Y), one of the main free amino acids in SHS (Zhang et al., 2018), has a strong absorbance peak at 280 nm due to its conjugated double bond. This may be the main contributor to the prominent sharp peak of F-IV with a corresponding MW of 186 Da, close to that of Y (181.19 Da).

3.2. Separation of antioxidant peptides by ultrafiltration and RP-HPLC

The antioxidant peptides in simulated GI digested SHS were separated using ultrafiltration and RP-HPLC. Fig. 1c-1f shows antioxidant activities of the ultrafiltration fractions of simulated GI digested SHS (SHS-I, SHS-II and SHS-III). The MW of those three fractions were > 10 kDa, 3-10

kDa and < 3 kDa, respectively. As shown in Fig. 1c-1f, all parameters representing antioxidant activities of the sample and its fractions, including DPPH radical scavenging activity, OH radical scavenging activity, Fe^{2+} chelating ability and reducing power, remarkably followed the order of SHS-III > SHS-II > SHS-I ($P < 0.05$) at the concentration of 5 mg/mL. These results indicate that the ultrafiltration fractions with lower MW had significantly higher antioxidant activity than the higher-MW fractions. Li, Wang, Chi, Gong, Luo, & Ding (2013) found that fractions with an average lower MW of fish collagen hydrolysate demonstrated significantly higher DPPH radical scavenging activity and reducing power. Centenaro, Salas-Mellado, Pires, Batista, Nunes, & Prentice (2014) also reported enhanced DPPH radical scavenging activity, OH radical scavenging capacity and reducing power from the ultrafiltration fractions of croaker hydrolysate with relatively low MW. Our result are in agreement with these previous reports. Therefore, the SHS-III was selected for further study due to its potent antioxidant activity.

SHS-III was further separated into ten fractions (F1-F10) using RP-HPLC and the result is illustrated in Fig. 1g. The DPPH radical scavenging activity of each fraction at the weight concentration of 2 mg/mL is exhibited in Fig. 1h. It can be seen that F9 showed the highest DPPH radical scavenging activity among all the fractions ($P < 0.05$). The DPPH radical scavenging activity of F9 was 59.99 ± 1.51%, about twice the lowest value (shown by F1) and 1/5 higher than the second-highest level (shown by F6 and F7) ($P < 0.05$). Hence, F9 derived from SHS-III was selected for further analysis.

3.3. Identification of antioxidant peptides by UPLC-MS/MS

The F9 fraction was then *de novo* sequenced using the UPLC-MS/MS system and 36 sequences

with abundance in MS/MS spectra above 1.00×10^7 were found. All sequences were obtained using the ProteinPilot 4.5 software and searched in the UniProt protein database. The sequencing results are exhibited in Table 1. It is shown that most of the searched sequences were from cytochrome, forkhead box P2, myocyte enhancer factor 2D, NADH-ubiquinone oxidoreductase and recombination activating protein. Eventually, four peptides (P1, P13, P17 and P31) were found with high sequencing confidence (> 85%) (Table 1) and considered as the finally identified antioxidant peptides. Their MS/MS spectra are exhibited in Fig. 2a-2d, and the corresponding sequence searching results are also shown in Table 1.

Typical antioxidative peptides are commonly small molecules containing 2-20 amino acid residues (Chen, Muramoto, Yamauchi, Fujimoto, & Nokihara, 1998). Previous studies demonstrated that MWs of antioxidant peptides derived from fish are commonly 500-1,500 Da (Centenaro et al., 2014; Nalinanon, Benjakul, Kishimura, & Shahidi, 2011). In this study, the identified antioxidant peptides had 8-17 amino acid residues with MW of approximately 0.8-1.7 kDa (Table 1 and Fig. 2), which is similar to previous reports (Centenaro et al., 2014; Chen et al., 1998; Nalinanon et al., 2011). Additionally, the high content of hydrophobic amino acid residues is another typical characteristic of high-antioxidant peptides (Ahmed, El-Bassiony, Elmalt, & Ibrahim, 2015). The percentage of highly hydrophobic residues in these identified peptides ranged from 40% (P17) to 88.24% (P13) with a chain length-weighted mean higher than 70%, which is consistent with published results about the antioxidant peptides (Puchalska, Marina, & García, 2014).

3.4. Synthesis and antioxidant activity evaluation of identified peptides

The identified peptides from the simulated GI digested SHS were synthesized and their

antioxidant properties were then determined. The DPPH radical scavenging activities and Fe^{2+} chelating abilities of these peptides are revealed in Fig. 2e and Fig. 2f, respectively, with the GSH, VC and/or EDTA as the control.

As displayed in Fig. 2e, P13 showed the highest DPPH radical scavenging activity among the identified peptides (IC_{50} = 1.39 ± 0.16 mM) ($P < 0.05$), which is comparable to that of the control GSH (IC_{50} = 1.24 ± 0.06 mM) ($P > 0.05$). The high content of hydrophobic residues (A, P, V, I, L, W, F, M and G) could be the main reason for its highest scavenging activity against DPPH radical among these peptides, since the DPPH radical is lipid-soluble and thus the high-hydrophobicity allows peptides to more readily react with lipid-soluble radicals (Pouzo, Descalzo, Zaritzky, Rossetti, & Pavan, 2016). Additionally, P17 exhibited the second highest DPPH radical scavenging activity (IC_{50} = 3.38 ± 1.67 mM) ($P < 0.05$), followed by P1 (IC_{50} = 8.06 ± 2.76 mM) ($P < 0.05$). However, P31 had the lowest DPPH radical scavenging activity among all these peptides (IC_{50} = 63.96 ± 6.47 and 89.87 ± 29.90 mM, respectively) ($P < 0.05$). The low scavenging activity against the DPPH radical may partially result from their relatively large MW and long molecular chain, since lower-MW and shorter peptides are more active as they act as electron donors and react with free radicals, rendering them more stable substances that stop chain reactions (Chi, Cao, Wang, Hu, Li, & Zhang, 2014; Halim, Yusof, & Sarbon, 2016).

As revealed in Fig. 2f, all the identified peptides showed significantly higher Fe^{2+} chelating ability than GSH (larger than 1 M) ($P < 0.05$). P17 exhibited the highest Fe^{2+} chelating activity among the identified peptides (IC_{50} = 4.60 ± 0.05 mM) ($P < 0.05$), which is comparable to that shown by the control EDTA (IC_{50} = 1.67 ± 0.05 mM) ($P > 0.05$). P1 and P31, closely followed P17, possessing the second-highest Fe^{2+} chelating activity with IC_{50} of about 7-26 mM ($P < 0.05$). However, P13 had the

lowest Fe^{2+} chelating ability among all the identified peptides (IC_{50} > 100 mM) ($P < 0.05$). Saiga, Tanabe, & Nishimura (2003) reported that the net-charged residues, including those negatively charged (acidic residues, D and E) and positively charged (basic residues, H, K and R), play a crucial role in Fe^{2+} and Cu^{2+} chelating abilities of peptides through electrostatic interactions. Therefore, P13, containing none net-charged residues, possessed the lowest Fe^{2+} chelating ability.

3.5. 3D structures and folding patterns of identified peptides

The most probable conformations and 3D structures of the identified peptides *de novo* are exhibited in Fig. S1, which were predicted by the PEP-FOLD tool V3.5. Results show that peptides possessed different folding patterns and spatial structures. It has been found that the predominant folding patterns of bioactive peptides mainly consist of β-turn (around 75% of total peptides) and α-helix (about 60%) rather than β-sheet and random coil (Kaur, Garg, & Raghava, 2007). Also, the α-helix plays a key role in the antioxidant capacity of peptides due to its contextual constraints (Jia, Natarajan, Forte, & Bielicki, 2002). Generally, all identified peptides had well-organized folding patterns including β-turn, β-sheet and/or α-helix except P31. Individually, P13 and P17 possessed 1-2 β-turns, while P1 and P13 had partial or intact α-helix whirls. However, the 3D structure of P31 was only displayed by the random coil, which may be another important reason for its relatively low scavenging activity against the DPPH radical (Fig. 2e).

3.6. Molecular docking of identified peptides with Keap1

The molecular docking analysis between identified antioxidant peptides and Keap1 was performed using the CDOCKER program of the Discovery Studio software 2016. The molecular docking models and results are shown in Fig. 3 and Table 2, respectively. The extent of binding

between identified antioxidant peptides and Keap1 should mainly be determined by the receptor active site, the –CDOCKER interaction energy (–CIE) score and the number of interacting amino acid residues (Wu, Du, Jia, & Kuang, 2016) (Table 2). Huerta et al. (2016) reported that the TX6 can effectively bind to Keap1, activate the Nrf2 and thus promote the backward ARE (anti-oxidation response element) expression. Hence, the TX6 was used as the reference to evaluate the binding degree between identified antioxidant peptides and Keap1. The molecular docking results show that almost all the identified peptide molecules successfully docked onto the active site of Keap1 except P31, which failed during the docking process (Table 2). The –CIE scores of P1, P13 and P17 were 72.04, 63.27 and 72.85 kJ/mol, respectively, whereas the –CIE score of TX6 was just 29.55 kJ/mol (Table 2). These three peptides had similar docking pockets with the TX6, which are located on the same active site of Keap1 (Fig. 3-A1, B1, C1 & D1).

Additionally, the TX6 established one hydrogen bond with GLY364 of Keap1 and six π bonds with TYR334, TYR525, ALA556 and TYR572 of Keap1 (Fig. 3-A2). However, there were more than eight amino acid residues involved in the interaction between P1, P13, P17 and Keap1 with larger numbers of hydrogen bonds and π bonds established compared with TX6 (Table 2 and Fig. 4). Individually, P1, P13 and P17 interacted with eight, sixteen and eleven amino acid residues of the Keap1 active site, respectively (Table 2). Moreover, in contrast with the TX6-Keap1 interaction, the interactions between these peptides and Keap1 were mainly hydrogen bonds rather than π bonds (Table 2 and Fig. 3). It has been reported that ligands interact with receptors via different intermolecular forces, such as hydrophobic, van der Waals's force, hydrogen bonds, π bonds and electrostatic interaction, among which hydrogen bonding interactions are probably the strongest (Miazaei, Mirdamadi, Ehsani, & Aminlari, 2018). All these results indicate that P1, P13 and P17 could

well bind to Keap1 with a binding complex even more stable than that of reference TX6.

3.7. Cytoprotective effects on cell damage induced by H_2O_2

The identified antioxidant peptides with successful molecular docking performance were further evaluated by a H_2O_2-induced oxidative stress cell model and the results are shown in Fig. 4. Fig. 4a, demonstrates that these peptides (125-1000 μM) had no significant toxicity effect on HepG2 cells compared with the control group ($P > 0.05$). Hydrogen peroxide penetrated cell membranes and caused cell damage. To evaluate the protective effect of identified peptides (P1, P13 and P17) against H_2O_2-induced cell damage, cells were pretreated with different concentrations of peptides (125-1000 μM) before being exposed to H_2O_2 (350 μg/mL). As illustrated in Fig. 4b, the cell viability of the damaged group significantly decreased to 43.40 ± 2.18% compared with the control group ($P < 0.05$). However, pretreatment of the identified peptides significantly increased cell viability to 60-82% ($P < 0.05$), and cell survival showed a remarkable dose-effect relationship with these peptides ($P < 0.05$). The results suggest that these synthesized peptides can significantly protect cells from H_2O_2-induced oxidative damage.

4. Conclusions

This work has achieved, for the first time, the identification and characterization of some antioxidant peptides from SHS generated from GI digestion. Specifically, four novel antioxidant peptides were separated, identified and characterized using ultrafiltration, RP-HPLC, UPLC-MS/MS, 3D structure *in silico* prediction, molecular docking analysis and H_2O_2-induced oxidative stress cell model. Results showed that the ultrafiltrated fraction with MW < 3 kDa (SHS-III), accounting for

about 77.96% (w/w) of the whole GI digested SHS, had the highest antioxidant capacity ($P < 0.05$). The antioxidant peptides in SHS-III were further separated into ten fractions by RP-HPLC and the F9 was selected for peptide identification due to its highest DPPH radical scavenging activity ($P < 0.05$). Among the identified peptides, PGMLGGSPPGLLGGSPP and SDGSNIHFPN showed high antioxidant activity which may be related to the contribution of 3D structure characteristics including β-turn and/or α-helix. The molecular docking study suggests that IVLPDEGK, PGMLGGSPPGLLGGSPP and SDGSNIHFPN can bind to the active site of Keap1 with the binding energy (–CIE > 60 kJ/mol) even higher than that of TX6 (–CIE = 29.55 kJ/mol). The cell viability assay also indicates that these three peptides had no cytotoxicity and could significantly protect cells from H_2O_2-induced oxidative damage. Thus, it can be concluded that the peptides with strong antioxidant activity generated from gastrointestinal digestion of SHS can promote *in vivo* antioxidant activity by participating in cellular anti-oxidation signaling pathways.

Acknowledgement

This research was financially supported by the National Natural Science Foundation of China (No. 31772047 and No. 31501495), the Fundamental Research Funds for the Central Universities of China (No. 2662019PY031) and the China Agriculture Research System (CARS-45-27).

Conflict of Interest

The authors have no conflict of interest.

References

1. Ahmed, A. S., El-Bassiony, T., Elmalt, L. M., & Ibrahim, H. R. (2015). Identification of potent antioxidant bioactive peptides from goat milk proteins. *Food Research International*, *74*, 80-88.
2. Centenaro, G. S., Salas-Mellado, M., Pires, C., Batista, I., Nunes, M. L., & Prentice, C. (2014). Fractionation of protein hydrolysates of fish and chicken using membrane ultrafiltration: investigation of antioxidant activity. *Applied Biochemistry and Biotechnology*, *172*(6), 2877-2893.
3. Chen, H. M., Muramoto, K., Yamauchi, F., Fujimoto, K., & Nokihara, K. (1998). Antioxidative properties of histidine-containing peptides designed from peptide fragments found in the digests of a soybean protein. *Journal of Agricultural and Food Chemistry*, *46*(1), 49-53.
4. Chi, C. F., Cao, Z. H., Wang, B., Hu, F. Y., Li, Z. R., & Zhang, B. (2014). Antioxidant and functional properties of collagen hydrolysates from Spanish mackerel skin as influenced by average molecular weight. *Molecules*, *19*(8), 11211-11230.
5. China Fishery Statistical Yearbook. (2019). China Fishery Statistical Yearbook. China Agricultural Press, Beijing, pp 31.
6. Decker, E. A., & Welch, B. (1990). Role of ferritin as a lipid oxidation catalyst in muscle food. *Journal of Agricultural and Food Chemistry*, *38*(3), 674-677.
7. Delgado, M. C. O., Nardo, A., Pavlovic, M., Rogniaux, H., Añón, M. C., & Tironi, V. A. (2016). Identification and characterization of antioxidant peptides obtained by gastrointestinal digestion of amaranth proteins. *Food Chemistry, 197,* 1160-1167.
8. Halim, N. R. A., Yusof, H. M., & Sarbon, N. M. (2016). Functional and bioactive properties of fish protein hydolysates and peptides: a comprehensive review. *Trends in Food Science &*

Technology, *51*, 24-33.

9. Han, J., Tang, S., Li, Y., Bao, W., Wan, H., Lu, C., Zhou, J., Li, Y., Cheong, L., & Su, X. (2018). *In silico* analysis and i*n vivo* tests of the tuna dark muscle hydrolysate anti-oxidation effect. *RSC advances*, *8*(25), 14109-14119.
10. Huerta, C., Jiang, X., Trevino, I., Bender, C. F., Ferguson, D. A., Probst, B., Swinger, K. K., Stoll, V. S., Thomas, P. J., Dulubova, I., Visnick, M., & Wigley, W. C. (2016). Characterization of novel small-molecule NRF2 activators: Structural and biochemical validation of stereospecific KEAP1 binding. *Biochimica et Biophysica Acta (BBA)-General Subjects*, *1860*(11), 2537-2552.
11. Jia, Z., Natarajan, P., Forte, T. M., & Bielicki, J. K. (2002). Thiol-bearing synthetic peptides retain the antioxidant activity of apolipoprotein A-I Milano. *Biochemical and Biophysical Research Communications*, *297*(2), 206-213.
12. Kaur, H., Garg, A., & Raghava, G. P. S. (2007). PEPstr: a de novo method for tertiary structure prediction of small bioactive peptides. *Protein and Peptide Letters*, *14*(7), 626-631.
13. Lamiable, A., Thévenet, P., Rey, J., Vavrusa, M., Derreumaux, P., & Tufféry, P. (2016). PEP-FOLD3: faster *de novo* structure prediction for linear peptides in solution and in complex. *Nucleic Acids Research*, *44*(W1), W449-W454.
14. Li, L., Liu, J., Nie, S., Ding, L., Wang, L., Liu, J., Liu, W., & Zhang, T. (2017). Direct inhibition of Keap1–Nrf2 interaction by egg-derived peptides DKK and DDW revealed by molecular docking and fluorescence polarization. *RSC Advances*, *7*(56), 34963-34971.
15. Li, Y., Jiang, B., Zhang, T., Mu, W., & Liu, J. (2008). Antioxidant and free radical-scavenging activities of chickpea protein hydrolysate (CPH). *Food Chemistry*, *106*(2), 444-450.
16. Li, Z., Wang, B., Chi, C., Gong, Y., Luo, H., & Ding, G. (2013). Influence of average molecular

506 weight on antioxidant and functional properties of cartilage collagen hydrolysates from *Sphyrna*
507 *lewini*, *Dasyatis akjei* and *Raja porosa*. *Food Research International*, *51*(1), 283-293.
508 17. Lowry, O. H., Rosebrough, N. J., Farr, A. L., & Randall, R. J. (1951). Protein measurement with
509 the Folin phenol reagent. *Journal of Biological Chemistry*, *193*(1), 265-275.
510 18. Magesh, S., Chen, Y., & Hu, L. (2012). Small molecule modulators of Keap1-Nrf2-ARE pathway
511 as potential preventive and therapeutic agents. *Medicinal Research Reviews*, *32*(4), 687-726.
512 19. Mirzaei, M., Mirdamadi, S., Ehsani, M. R., & Aminlari, M. (2018). Production of antioxidant and
513 ACE-inhibitory peptides from *Kluyveromyces marxianus* protein hydrolysates: Purification and
514 molecular docking. *Journal of Food and Drug Analysis*, *26*(2), 696-705.
515 20. Nalinanon, S., Benjakul, S., Kishimura, H., & Shahidi, F. (2011). Functionalities and antioxidant
516 properties of protein hydrolysates from the muscle of ornate threadfin bream treated with pepsin
517 from skipjack tuna. *Food Chemistry*, *124*(4), 1354-1362.
518 21. Oyaizu, M. (1986). Studies on products of browning reaction: antioxidative activity of products
519 of browning reaction. *Japanese Journal of Nutrition*, *44*(6), 307-315.
520 22. Pouzo, L. B., Descalzo, A. M., Zaritzky, N. E., Rossetti, L., & Pavan, E. (2016). Antioxidant
521 status, lipid and color stability of aged beef from grazing steers supplemented with corn grain and
522 increasing levels of flaxseed. *Meat Science*, *111*, 1-8.
523 23. Puchalska, P., Marina, M. L., & García, M. C. (2014). Isolation and identification of antioxidant
524 peptides from commercial soybean-based infant formulas. *Food Chemistry*, *148*, 147-154.
525 24. Sahid, N. A., Hayati, F., Rao, C. V., Ramely, R., Sani, I., Dzulkarnaen, A., Zakaria, Z., Hassan, S.,
526 Zahari, A., & Ali, A. A. (2018). Snakehead consumption enhances wound healing? From tradition
527 to modern clinical practice: a prospective randomized controlled trial. *Evidence-Based*

Complementary and Alternative Medicine, 2018.

25. Saiga, A. I., Tanabe, S., & Nishimura, T. (2003). Antioxidant activity of peptides obtained from porcine myofibrillar proteins by protease treatment. *Journal of Agricultural and Food Chemistry, 51*(12), 3661-3667.
26. Schäfer, M., & Werner, S. (2008). Oxidative stress in normal and impaired wound repair. *Pharmacological research*, *58*(2), 165-171.
27. Shen, S., Chahal, B., Majumder, K., You, S. J., & Wu, J. (2010). Identification of novel antioxidative peptides derived from a thermolytic hydrolysate of ovotransferrin by LC-MS/MS. *Journal of Agricultural and Food Chemistry*, *58*(13), 7664-7672.
28. Sheng, J., Yang, X., Chen, J., Peng, T., Yin, X., Liu, W., Liang, M., Wan, J., & Yang, X. (2019). Antioxidative effects and mechanism study of bioactive peptides from defatted walnut (*Juglans regia L.*) meal hydrolysate. *Journal of Agricultural and Food Chemistry*, *67*(12), 3305-3312.
29. Sila, A., & Bougatef, A. (2016). Antioxidant peptides from marine by-products: Isolation, identification and application in food systems. A review. *Journal of Functional Foods, 21*, 10-26.
30. Venkatesan, J., Anil, S., Kim, S. K., & Shim, M. S. (2017). Marine fish proteins and peptides for cosmeceuticals: A review. *Marine drugs, 15*(5), 143.
31. Wahab, S. Z. A., Kadir, A. A., Hussain, N. H. N., Omar, J., Yunus, R., Baie, S., Mohd, N. N., Idiana, H. I., Mahmood, W. H. W., Razak, A. A., & Yusoff, W. Z. W. (2015). The effect of *Channa striatus* (Haruan) extract on pain and wound healing of post-lower segment caesarean section women. *Evidence-Based Complementary and Alternative Medicine, 2015*.
32. Wang, C. H., Doan, C. T., Nguyen, V. B., Nguyen, A. D., & Wang, S. L. (2019). Reclamation of fishery processing waste: A mini-review. *Molecules, 24*(12), 2234.

33. Wu, F., Zhang, G., Huo, Y., Xiong, S., & Du, H. (2018). Rheology and Texture Properties of Surimi Gels of Northern Snakehead (*Channa Argus*) as Affected by *Angelica Sinensis* (Oliv.) Diels. (Danggui) Powder. *Journal of Aquatic Food Product Technology, 27*(4), 486-495.

34. Wu, Q., Du, J., Jia, J., & Kuang, C. (2016). Production of ACE inhibitory peptides from sweet sorghum grain protein using alcalase: Hydrolysis kinetic, purification and molecular docking study. *Food Chemistry, 199*, 140-149.

35. Zhang, D. D., Lo, S. C., Sun, Z., Habib, G. M., Lieberman, M. W., & Hannink, M. (2005). Ubiquitination of Keap1, a BTB-Kelch substrate adaptor protein for Cul3, targets Keap1 for degradation by a proteasome-independent pathway. *Journal of Biological Chemistry, 280*(34), 30091-30099.

36. Zhang, J., Du, H., Zhang, G., Kong, F., Hu, Y., Xiong, S., & Zhao, S. (2020). Identification and characterization of novel antioxidant peptides from crucian carp (*Carassius auratus*) cooking juice released in simulated gastrointestinal digestion by UPLC-MS/MS and *in silico* analysis. *Journal of Chromatography B*, 1136, 121893.

37. Zhang, G., Zheng, S., Feng, Y., Shen, G., Xiong, S., & Du, H. (2018). Changes in nutrient profile and antioxidant activities of different fish soups, before and after simulated gastrointestinal digestion. *Molecules*, *23*(8), 1965.

38. Zhang, T., Li, Y., Miao, M., & Jiang, B. (2011). Purification and characterisation of a new antioxidant peptide from chickpea (*Cicer arietium L.*) protein hydrolysates. *Food Chemistry, 128*(1), 28-33.

39. Zheng, L., Ren, J., Su, G., Yang, B., & Zhao, M. (2013). Comparison of in vitro digestion characteristics and antioxidant activity of hot-and cold-pressed peanut meals. *Food Chemistry,*

572 *141*(4), 4246-4252.

573 40. Zuraini, A., Somchit, M. N., Solihah, M. H., Goh, Y. M., Arifah, A. K., Zakaria, M. S., Somchit,

574 N., Rajion, M. A., Zakaria, Z. A., & Jais, A. M. M. (2006). Fatty acid and amino acid composition

575 of three local Malaysian Channa spp. fish. *Food Chemistry, 97*(4), 674-678.

576 **Table 1 Sequencing results of antioxidant peptides in F9 from the simulated GI digested SHS**

Protein source[a]	Peptide No.	Calculated mass (Da)	Observed mass (Da)	Sequence	Abundance in spectra	Confidence of sequencing (%)
A1-antitrypsin	**P1**	**869.4922**	**869.4858**	**IVLPDEGK**	**1.01×10^{8}**	**94.55**
Cystic fibrosis transmembrane conductance regulator	P2	1358.6300	1358.7153	SVEGGQSVGLLGRT	2.70×10^{7}	33.83
Cytochrome	P3	2164.0630	2164.1423	WNLGSLLGLCLVAQLMTGLF	6.20×10^{7}	79.18
	P4	1972.9020	1972.9530	EEAGAGTGWTVYPPLAGNLA	1.01×10^{8}	66.25
	P5	2027.9430	2028.0316	GVEAGVGTGWTVYPPLAGNLA	9.60×10^{7}	21.05
	P6	869.4921	869.47930	LTIKAMGH	1.50×10^{8}	54.94
Doublesex- and mab-3-related transcription factor 5	P7	1141.5580	1141.5590	SRGLAFMTPY	3.30×10^{7}	60.13
Early growth response 2B	P8	2475.2050	2475.2144	GPGGGGGGSEGGPPRLPSAYSPQNLPL	1.30×10^{7}	46.86
Estrogen receptor β	P9	1585.7190	1585.8173	SAQSRTGGSKPKTGPAG	2.70×10^{7}	29.11
Forkhead box P2	P10	1590.7860	1590.8076	PGMLGGSPPGLLGGSPPT	6.00×10^{7}	74.55
	P11	1054.6080	1054.5481	MPQVPSVLGGA	8.50×10^{7}	44.60
	P12	1277.5860	1277.6438	PGMLGGSPPGLLGGS	1.36×10^{8}	15.43
	P13	**1505.7010**	**1505.7548**	**PGMLGGSPPGLLGGSPP**	**1.56×10^{8}**	**99.00**
	P14	1708.8100	1708.8818	MPQVPSVLGGANVPSIGA	8.00×10^{7}	51.03
	P15	926.5137	926.4896	MPQVPSVLG	4.00×10^{7}	21.20
	P16	1523.7160	1523.6675	TGPMGGSCHGLLGGDPS	2.50×10^{7}	33.93
Galectin	**P17**	**1086.4800**	**1086.4730**	**SDGSNIHFPN**	**1.56×10^{8}**	**89.60**
Muellerian-inhibiting factor	P18	1136.5230	1136.5714	SPASSQTLSFL	1.20×10^{8}	41.71
Myocyte enhancer factor 2D	P19	1379.7060	1379.7521	GLPQRPASAGALLGG	9.50×10^{7}	25.71

	P20	1450.7490	1450.7528	NTVSPGLPQRPASAG	8.10×10^{7}	33.95
NADH-ubiquinone oxidoreductase	P21	883.5083	883.5167	PFGLLQPI	8.50×10^{7}	38.01
	P22	939.5437	939.5753	GLVAGGILIQ	8.00×10^{7}	33.97
	P23	1155.6550	1155.6288	IQTPWGLTGAL	8.50×10^{7}	45.64
	P24	1222.6260	1222.6809	GSIISGLLITSY	4.00×10^{7}	40.02
	P25	1651.9040	1651.8756	MVAIGLNQPQLAFLH	8.20×10^{7}	53.25
	P26	1170.6170	1170.6860	TAIGLLASLELA	1.50×10^{7}	81.02
	P27	1620.7920	1620.8148	GLAAVASNPSPYYAALG	2.80×10^{7}	31.63
Prolactin receptor	P28	1646.7970	1646.7020	DKSGAPKEEQDNGSGE	8.20×10^{7}	28.20
Proliferating cell nuclear antigen	P29	883.5083	883.4651	VEQLGIPE	8.00×10^{7}	37.26
Recombinase	P30	853.5096	853.5273	ALTAVLGPI	1.16×10^{8}	37.96
Recombination activating protein	**P31**	**1722.8330**	**1722.8424**	**SVSIRADGGEGEVTVFT**	$\mathbf{6.50\times10^{7}}$	**95.35**
	P32	1208.6110	1208.6877	AVLGPIVAERNA	8.50×10^{7}	51.87
	P33	2005.9590	2005.9312	AEPQPNSELSCKPLCLMF	1.00×10^{8}	70.93
Si:dkey-174m14.3	P34	1272.6150	1272.5444	WVGASPSPECSPG	2.50×10^{7}	35.16
Sorting nexin 33	P35	1182.5710	1182.5305	LGPQWNENPQ	6.00×10^{7}	69.08
Transferrin receptor 1	P36	1149.5320	1149.5455	WGPGFAASTVGT	9.10×10^{7}	44.07

[a] The protein sources of the identified peptides are from the UniProt protein database.

578 **Table 2 Molecular docking results of identified peptides from the simulated GI digested SHS with Keap1**

Ligand	Sequence	–CIE [a] (kJ/mol)	Interactions with Keap1	Number of hydrogen bonds	Number of π bonds
TX6	(6aS,7S,10aS)-8-hydroxy-4-methoxy-2,7,10a-trimethyl-5,6,6a,7,10,10a-hexahydrobenzo[h]quinazoline-9-carbonitrile	29.5522	TYR334, GLY364, TYR525, ALA556, TYR572	1	6
P1	IVLPDEGK	72.0357	ARG380, ARG415, HIS436, ILE461, ARG483, SER508, SER555, TYR572	9	1
P13	PGMLGGSPPGLLGGSPP	63.2653	GLY364, LEU365, ALA366, ARG380, ASN382, ARG415, ILE416, GLY433, ARG483, CYS434, ALA510, TYR525, LEU557, TYR572, GLY603, VAL604	17	2
P17	SDGSNIHFPN	72.8495	LEU365, ARG380, ARG415, GLY462, ARG483, ALA510, TYR525, ALA556, LEU557, TYR572, GLY603	11	4
P31	SVSIRADGGEGEVTVFT	—	—	—	—

579 [a] –CIE, –CDOCKER interaction energy.

Figure captions

Fig. 1. The MW distribution (a-b) and separation (c-h) of antioxidant peptides from the simulated GI digested SHS. a-b, the MW distribution of peptides from simulated GI digested SHS by gel filtration chromatography (a) and the standard curve of lg (MW)-elution time relationship (b). The whole SHS digesta can be divided into four fractions (F-I to F-IV) by MW distribution. c-f, the DPPH radical scavenging activity (c), OH radical scavenging activity (d), Fe^{2+} chelating ability (e) and reducing power (f) of the simulated GI digested SHS and its ultrafiltration fractions. Different lowercases above the error bar denote significant differences among antioxidant activities of the simulated digested SHS sample and its different fractions ($P < 0.05$). The MWs of SHS-I, SHS-II and SHS-III were > 10 kDa, 3-10 kDa and < 3 kDa, respectively. The concentration of all samples used in the detection was 5 mg/mL. g-h, RP-HPLC chromatogram of peptides in SHS-III (g) and the DPPH radical scavenging activities of its further separated fractions (F1 to F10) (h). Different lowercases above the error bar denote significant differences among DPPH radical scavenging activities of different fractions ($P < 0.05$). The concentration of all fractions used was 2 mg/mL.

Fig. 2. The MS/MS spectra (a-d) and antioxidant activities (e-f) of the identified and synthesized peptides. a-d, MS/MS spectra of the five identified antioxidant peptides. a, P1, IVLPDEGK; b, P13, PGMLGGSPPGLLGGSPP; c, P17, SDGSNIHFPN; d, P31, SVSIRADGGEGEVTVFT. The upper and lower dash labeled the b ion and y ion, respectively. e-f, the DPPH radical scavenging activity (e) and Fe^{2+} chelating ability (f) of synthesized antioxidant peptides. Different lowercases above the error bar denote significant differences among the identified antioxidant peptides from the simulated GI digested SHS ($P < 0.05$).

Fig. 3. Molecular docking model of interactions between identified antioxidant peptides and Keap1 (PDB ID: 2FLU). The TX6 (Pub Chem ID: 121488089) was used as a reference. Ligand code: A, TX6; B, P1, IVLPDEGK; C, P13, PGMLGGSPPGLLGGSPP; D, P17, SDGSNIHFPN. A1, B1, C1 and D1, the ligand molecule was bound to the integral Keap1. A2, B2, C2 and D2, the 2D diagram of interactions between the ligand molecule and active amino acid residues of Keap1.

Fig. 4. Protective effects of synthesized antioxidant peptides against H_2O_2-induced stress damage in HepG2 cells. a, the cell viability of different concentrations of synthetic peptides on HepG2 cells. b, Protective effects of different concentrations of P1, P13 and P17 on H_2O_2-induced damage of HepG2 cells. Different lowercases above the error bar denote significant differences among various synthetic antioxidant peptides with different concentrations (125-1000 μM) ($P < 0.05$).

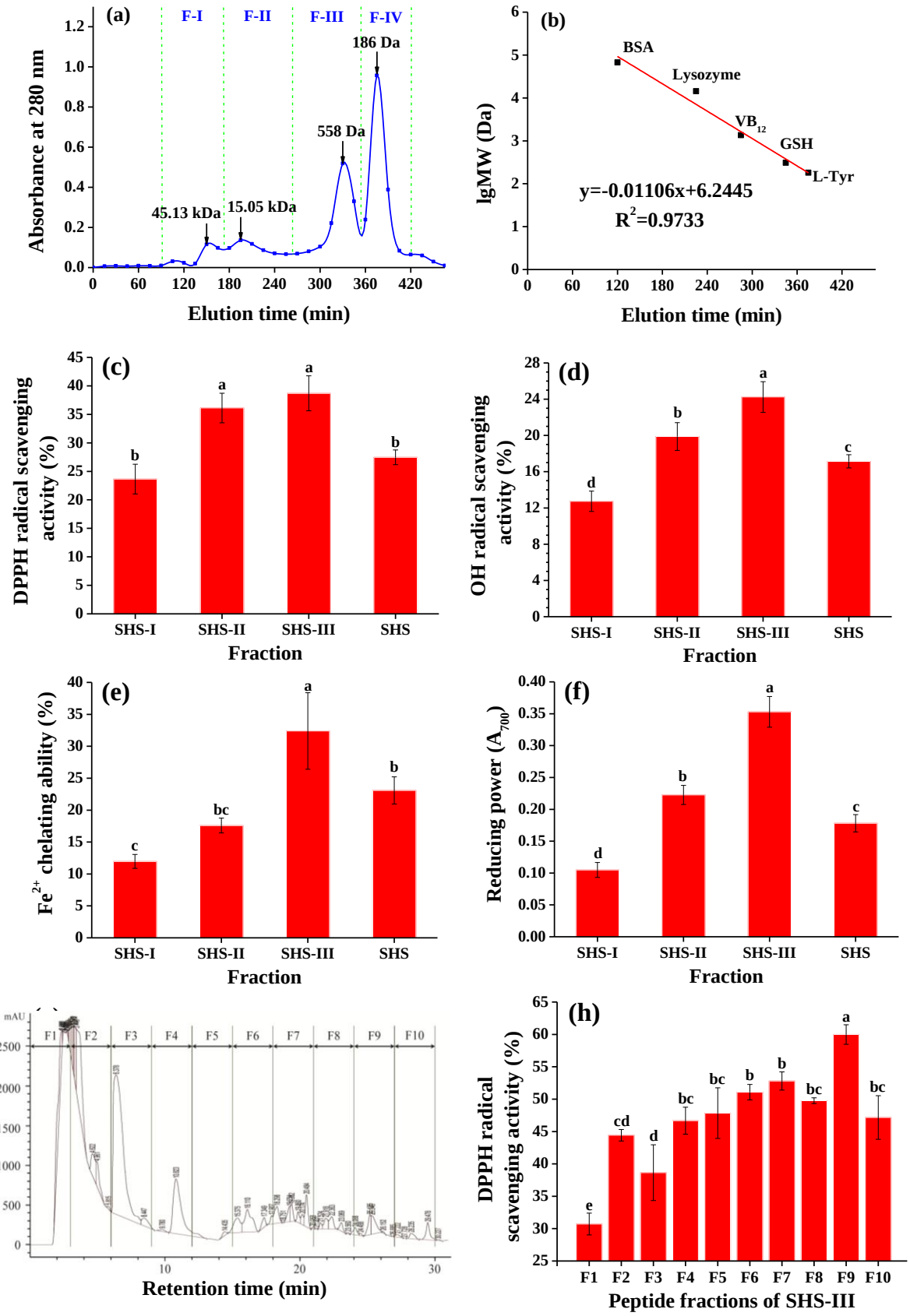
(a)
F-I
F-II
F-III
F-IV
186 Da
558 Da
45.13 kDa
15.05 kDa
Absorbance at 280 nm
Elution time (min)
(b)
BSA
Lysozyme
VB12
GSH
L-Tyr
y=-0.01106x+6.2445
R2=0.9733
lgMW (Da)
Elution time (min)
(c)
DPPH radical scavenging activity (%)
SHS-I
SHS-II
SHS-III
SHS
Fraction
(d)
OH radical scavenging activity (%)
Fraction
(e)
Fe2+ chelating ability (%)
Fraction
(f)
Reducing power (A700)
Fraction
mAU
F1
F2
F3
F4
F5
F6
F7
F8
F9
F10
Retention time (min)
(h)
DPPH radical scavenging activity (%)
Peptide fractions of SHS-III

Fig. 1

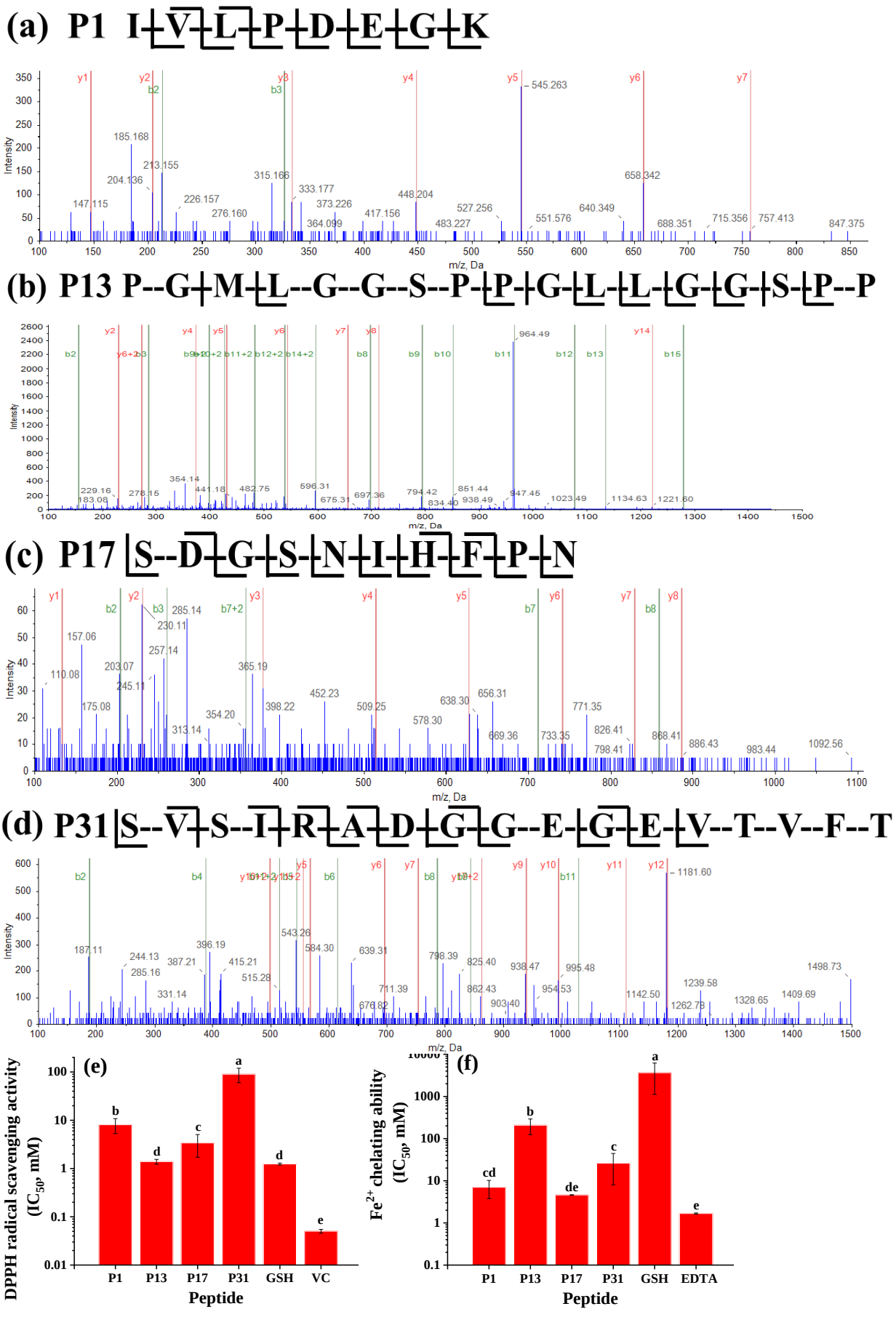
(a) P1 I-V-L-P-D-E-G-K
(b) P13 P--G-M-L--G--G--S--P-P-G-L-L-G-G-S-P--P
(c) P17 S--D-G-S-N-I-H--F-P-N
(d) P31 S--V-S--I-R-A-D-G-G--E-G-E-V--T--V--F--T
Intensity
m/z, Da
(e)
DPPH radical scavenging activity (IC50, mM)
(f)
Fe2+ chelating ability (IC50, mM)
P1
P13
P17
P31
GSH
VC
EDTA
Peptide

Fig. 2

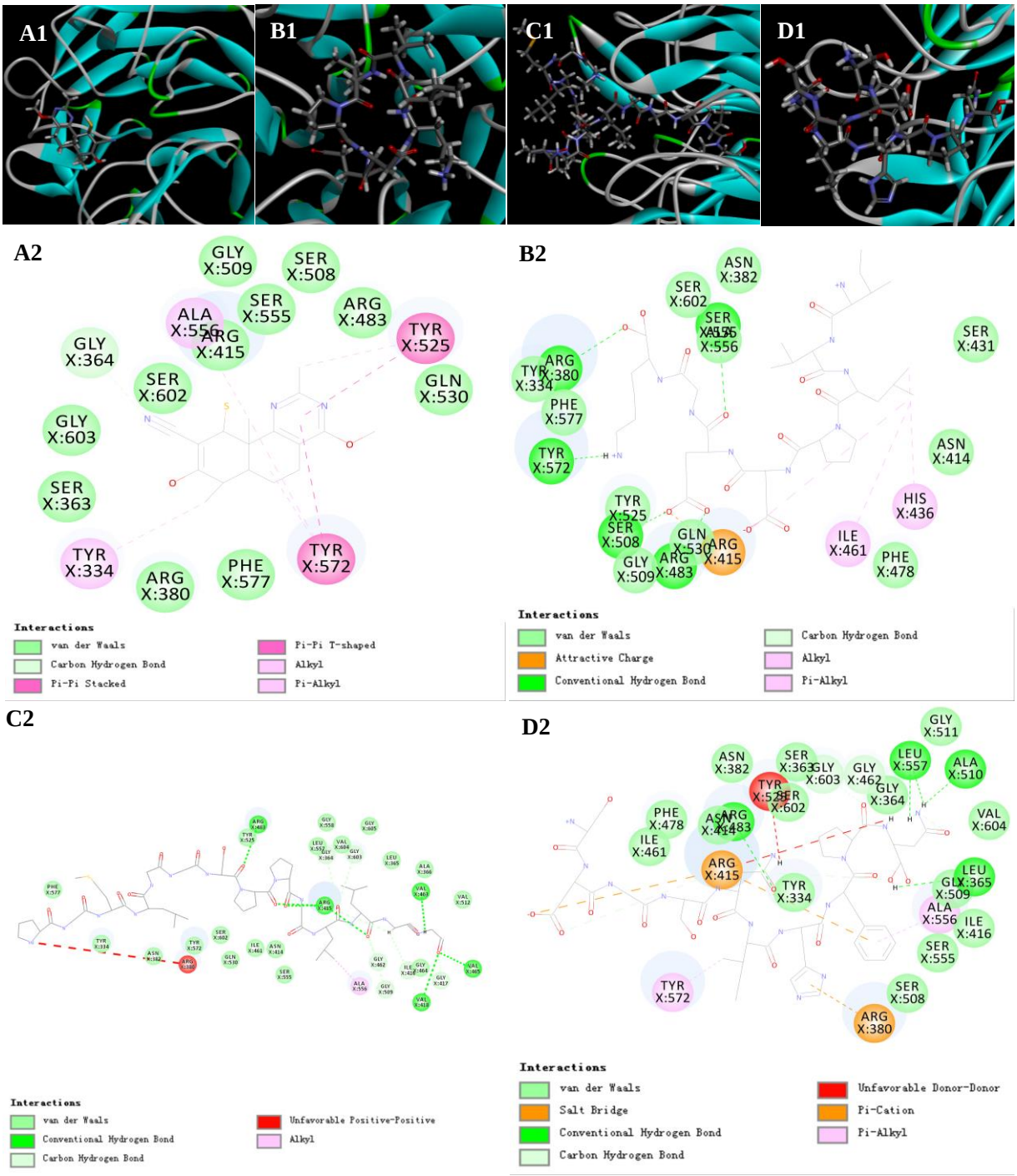
A1
B1
C1
D1
A2
GLY X:509
SER X:508
SER X:555
ALA X:556
ARG X:415
ARG X:483
TYR X:525
GLN X:530
GLY X:364
SER X:602
GLY X:603
SER X:363
TYR X:334
ARG X:380
PHE X:577
TYR X:572
Interactions
van der Waals
Pi-Pi T-shaped
Carbon Hydrogen Bond
Alkyl
Pi-Pi Stacked
Pi-Alkyl
B2
ASN X:382
SER X:602
SER X:556
SER X:431
ARG X:380
TYR X:334
PHE X:577
TYR X:572
ASN X:414
TYR X:525
HIS X:436
SER X:508
GLN X:530
ARG X:415
ILE X:461
GLY X:509
ARG X:483
PHE X:478
Interactions
van der Waals
Carbon Hydrogen Bond
Attractive Charge
Alkyl
Conventional Hydrogen Bond
Pi-Alkyl
C2
Interactions
van der Waals
Unfavorable Positive-Positive
Conventional Hydrogen Bond
Alkyl
Carbon Hydrogen Bond
D2
GLY X:511
ASN X:382
SER X:363
GLY X:603
GLY X:462
LEU X:557
ALA X:510
TYR X:525
SER X:602
GLY X:364
PHE X:478
ASN X:414
VAL X:604
ILE X:461
ARG X:415
TYR X:334
LEU X:365
GLY X:509
ALA X:556
ILE X:416
SER X:555
TYR X:572
SER X:508
ARG X:380
Interactions
van der Waals
Unfavorable Donor-Donor
Salt Bridge
Pi-Cation
Conventional Hydrogen Bond
Pi-Alkyl
Carbon Hydrogen Bond

Fig. 3

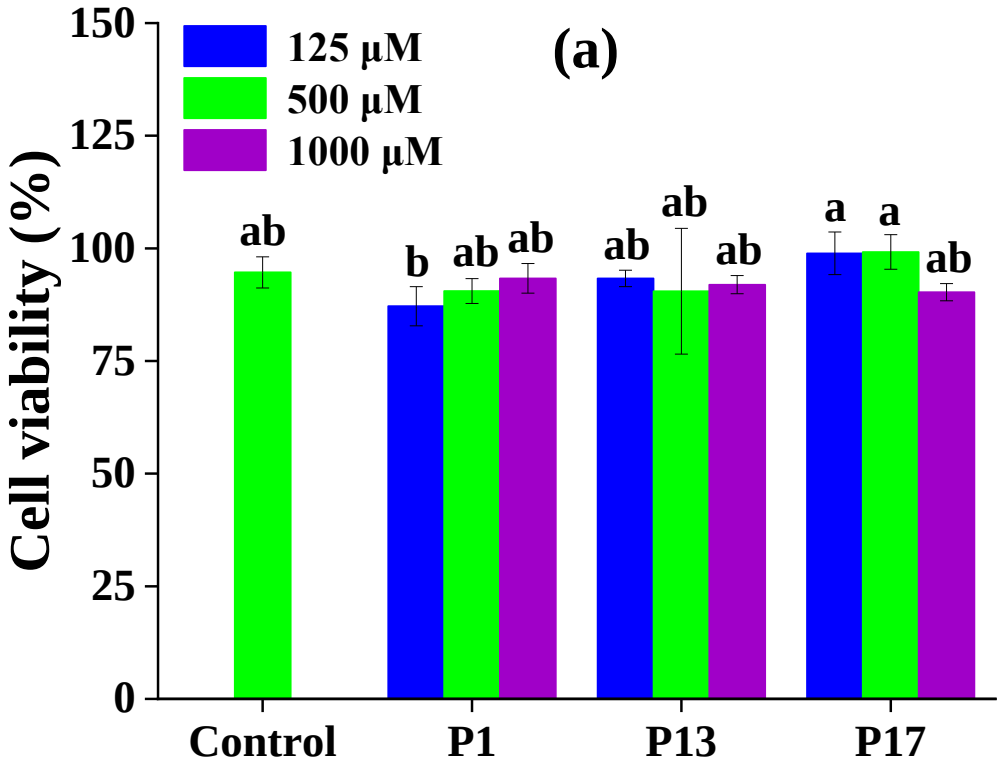

647

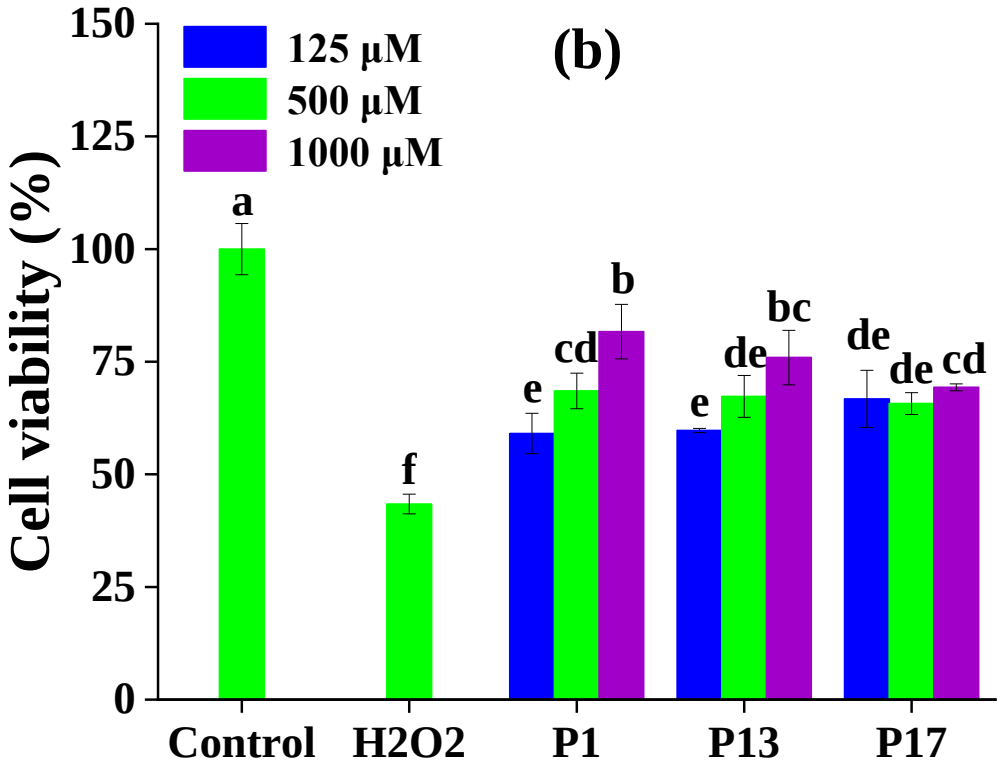

648

649 **Fig. 4**